Preprints.org

Article

Not peer-reviewed version

Detection of Hepatitis C Virus Infection from Patient Sera in Cell Culture Using Semi-Automated Image Analysis

Noemi Schäfer , Paul Rothhaar , Christian Heuss , Christoph Neumann-Haefelin , Robert Thimme , Julia Dietz , Christoph Sarrazin , Paul Schnitzler , Uta Merle , Sofía Pérez-del-Pulgar , Vibor Laketa , Volker Lohmann *

Posted Date: 25 October 2024

doi: 10.20944/preprints202410.2010.v1

Keywords: HCV; patient sera; cell culture; image analysis; infection; machine learning

Preprints.org is a free multidisciplinary platform providing preprint service that is dedicated to making early versions of research outputs permanently available and citable. Preprints posted at Preprints.org appear in Web of Science, Crossref, Google Scholar, Scilit, Europe PMC.

Copyright: This open access article is published under a Creative Commons CC BY 4.0 license, which permit the free download, distribution, and reuse, provided that the author and preprint are cited in any reuse.

Preprints.org (www.preprints.org) | NOT PEER-REVIEWED | Posted: 25 October 2024 doi:10.20944/preprints202410.2010.v1

Disclaimer/Publisher's Note: The statements, opinions, and data contained in all publications are solely those of the individual author(s) and contributor(s) and not of MDPI and/or the editor(s). MDPI and/or the editor(s) disclaim responsibility for any injury to people or property resulting from any ideas, methods, instructions, or products referred to in the content.

Article

Detection of Hepatitis C Virus Infection from Patient Sera in Cell Culture Using Semi-Automated Image Analysis

Noemi Schäfer [1], Paul Rothhaar [1], Christian Heuss [1], Christoph Neumann-Haefelin [2], Robert Thimme [2], Julia Dietz [3,4], Christoph Sarrazin [3,4,5], Paul Schnitzler [6], Uta Merle [7], Sofía Pérez-del-Pulgar [8], Vibor Laketa [6,9] and Volker Lohmann [1,9,*]

[1] Department of Infectious Diseases, Molecular Virology, Section virus-host interactions, Heidelberg University, Heidelberg, Germany
[2] Department of Medicine II, Medical Center, University of Freiburg, Freiburg, Germany
[3] Department of Internal Medicine 1, University Hospital, Goethe University, Frankfurt, Germany
[4] German Center for Infection Research (DZIF), Partner Site Frankfurt, Frankfurt, Germany
[5] Medizinische Klinik 2, St. Josefs-Hospital, Wiesbaden, Germany
[6] Department of Infectious Diseases, Virology, University Hospital Heidelberg, Heidelberg, Germany
[7] Department of Internal Medicine IV, University Hospital Heidelberg, Heidelberg, Germany
[8] Liver Unit, Hospital Clínic, IDIBAPS and CIBEREHD, University of Barcelona, Barcelona, Spain
[9] German Center for Infection Research (DZIF), Partner Site Heidelberg, Heidelberg, Germany
* Correspondence: Volker.lohmann@med.uni-heidelberg.de

Abstract: The study of hepatitis C virus (HCV) replication in cell culture is mainly based on cloned viral isolates requiring adaptation for efficient replication in Huh7 hepatoma cells. The analysis of wild type (WT) isolates has been enabled by expression of SEC14L2 and by inhibitors targeting deleterious host factors. Here, we aimed at optimizing cell culture models to allow infection with HCV from patient sera. We used Huh7-Lunet cells ectopically expressing SEC14L2, CD81 and a GFP reporter with nuclear translocation upon cleavage by the HCV protease to study HCV replication, combined with a drug-based regimen for stimulation of non-modified wildtype isolates. RT-qPCR based quantification of HCV infections using patient sera suffered from high background in the daclatasvir treated controls. We therefore established an automated image analysis pipeline based on imaging of whole wells and iterative training of a machine-learning tool, using nuclear GFP localization as a readout for HCV infection. Upon visual validation of hits assigned by the automated image analysis the method revealed no background in daclatasvir treated samples. Thereby, infection events were found for 15 of 34 high titer HCV genotype (gt) 1b sera, revealing a significant correlation of serum titer and successful infection. We further show that transfection of viral RNA extracted from sera can be used in this model as well, albeit with so far limited efficiency. Overall, we generated a robust serum infection assay for gt1b isolates using semi-automated image analysis, which was superior to conventional RT-qPCR based quantification of viral genomes.

Keywords: HCV; patient sera; cell culture; image analysis; infection; machine learning

Introduction

Around 58 million people are chronically infected with HCV worldwide, leading to approximately 300,000 deaths per year (WHO, 2021). HCV is a positive single-strand, enveloped RNA virus from the family of *Flaviviridae* with a genome length of around 9600 nucleotides. Upon infection with HCV, the virus replicates in human liver cells, leading to a chronic infection in around 60 to 85% of cases [1], resulting often in severe liver disease, including cirrhosis and hepatocellular carcinoma (HCC) [2,3]. The high error rate of the viral polymerase leads to a huge genetic heterogeneity of HCV genomes, which are now grouped into 8 HCV genotypes (gt) with up to 30% sequence difference and numerous subtypes [4–6]. Even within one single patient, HCV exhibits a

© 2024 by the author(s). Distributed under a Creative Commons CC BY license.

Preprints.org (www.preprints.org) | NOT PEER-REVIEWED | Posted: 25 October 2024 doi:10.20944/preprints202410.2010.v1

quasi-species nature with many heterogeneous viral genomes found in the same person [7], which is a major hindrance for the development of a protective vaccine. The introduction of direct acting antivirals (DAAs) from 2011 on revolutionized HCV treatment, meanwhile reaching sustained virologic response rates (SVRs) far above 90% [8]. So far, the emergence of resistance-associated substitutions (RAS) against DAAs has been of limited impact (reviewed in [9,10]), but might gain importance in the future with the emergence of new virus strains and subtypes [11]. On the long run, a prophylactic vaccine against the virus is the ultimate goal to reach, being the most effective and least cost-intensive tool to globally extinct HCV (reviewed in [9]).

The HCV subgenomic replicon system was the first HCV cell culture model, allowing studies on the virus in a laboratory context [12]. It was later discovered, that the successful replication of this isolate named Con1 was based on conserved acquired mutations, which were not present in the original sequence [13]. Nowadays, a wide range of reporter replicons as well as cell culture adapted full length strains with the capability of producing infectious particles are available for many different genotypes, but all based on cloned viral isolates [14–20]. However, until now culturing WT HCV virus from patient serum remains difficult, thereby hampering studies on natural heterogeneity of HCV quasi-species and their functional implications.

Progress in the field of HCV WT replication in cell culture has been made due to essential findings concerning two cellular host factors, namely Phosphatidylinositol 4-kinase IIIα (PI4KA) and SEC14L2. PI4KA is a cellular lipid kinase present in primary hepatocytes as well as in the Huh7 cell lines mainly used for culturing HCV. However, in contrast to healthy hepatocytes, PI4KA is overexpressed in hepatoma cell lines [21,22]. It could be shown, that a combined, limited chemical inhibition of PI4KA and Casein kinase I alpha (CKIa) [23] phenocopied the effect of distinct cell culture adaptive mutations in the viral proteins NS5A and NS5B [21]. This so-called PCi treatment thereby facilitated replication of HCV gt1b WT sequences in Huh7 cells [24]. SEC14L2 is a cytosolic lipid-exchange protein, which is expressed in primary human hepatocytes, but not in Huh7 cells. It was discovered as cellular host factor supporting replication of HCV WT pan-genotypically in a screen using Huh7.5 cells expressing a cDNA-library [25]. However, overexpression of SEC14L2 in Huh7 cells acts most efficiently on gt1b and has a variable effects on replication levels of other gts [26].

Replication of HCV WT isolates from patient serum using either PCi treatment or SEC14L2 overexpression could be achieved for a small number of sera, mainly with high titers obtained from patients after liver transplantation [21,25,26]. We further found that a combination of PCi treatment and SEC14L2 overexpression resulted in additive effects in enhancing replication of two gt1b WT replicons in Huh7 Lunet cells [24], but potential benefits in culturing serum-derived virus remained unexplored.

Here, we aimed at establishing a cell culture model for studying replication of serum-derived HCV. We generated a robust infection assay for gt1b isolates based on cells expressing SEC14L2 and PCi treatment. The detection of HCV-protease dependent nuclear localization of GFP, analysed by whole well imaging and automated image analysis with visual validation of positive cells was proven to be superior to conventional RT-qPCR based quantification of viral genomes.

Materials and Methods

Cell Culture:

Huh7 Lunet CD81H/MGN/SEC14L2 (Huh7 cell line overexpressing the entry factor CD81, SEC14L2 and additionally harbouring a MAVS-GFP-NLS-reporter system with blasticidin, puromycin and neomycin as selection markers) have been described previously [24]; Huh7 LucUbiNeo Con1 ET [27]); Huh7 LucUbiNeo JFH [28] have been described previously. Huh7 LucUbiNeo GLT1 cells were generated by electroporation of in vitro transcribed RNA generated from plasmid pFK i389 LucUbiNeo NS3-3′ GLT1 WT into Huh7-Lunet cells stably expressing SEC14L2, followed by selection with 500 µg/ml G418.

Preprints.org (www.preprints.org) | NOT PEER-REVIEWED | Posted: 25 October 2024 doi:10.20944/preprints202410.2010.v1

Cells were cultured in complete Dulbecco´s modified Eagle's medium (DMEM) supplemented with 2 mM L-glutamine, 0.1 mM nonessential amino acids, 100 U/ml of penicillin, 100 mg/ml of streptomycin (all Gibco) and 10% fetal calf serum (FCS) at 37 °C and 5% (v/v) CO_2. Medium of cells harbouring selectable replicons was supplemented with 500 µg/ml G418.

Huh7-Lunet CD81H/MGN/SEC14L2 (Huh7-Lunet C/M/S) cells were cultured in presence of G418 (1 mg/ml), puromycin (2 µg/ml) and blasticidin (5 µg/ml) to maintain transgene expression in all cells.

Plasmids:

For replication studies, gt1b subgenomic replicons (SGRs) with a luciferase reporter were used and have been described previously: pFK i341 PiLuc NS3-3′ Con1, pFK i341 PiLuc NS3-3′ Con1 ΔGDD (Replication deficient negative control) [12,13]); and pFK i341 PiLuc NS3-3′ GLT1 [24]. To generate cell lines stably harbouring the GLT1 SGR, pFK i389 LucUbiNeo NS3-3′ GLT1 WT was generated by replacing the NS3-3′ region of the respective Con1 replicon [29] by the GLT1 sequence. For production of infectious virus, constructs harbouring the full viral sequence were used: pFK JC1 [16], pUC DBN WT [20] and pUC TN WT [19].

Patient Material and Ethics Statement:

All patient sera used in this study were obtained from Julia Dietz and Christoph Sarrazin (German Center for Infection Research (DZIF), External Partner Site, Frankfurt, Germany), Uta Merle (University Hospital Heidelberg, Department of Gastroenterology, Heidelberg, Germany), Christoph Neumann-Haefelin and Robert Thimme (University of Freiburg, Department of Medicine, Freiburg Germany), Sofía Pérez-del-Pulgar [30] (University of Barcelona, Liver Unit, Hospital Clínic, IDIBAPS, CIBERehd, Barcelona, Spain) and Paul Schnitzler (University of Heidelberg, Department of Infectious Diseases, Virology, Heidelberg, Germany). The use of the patient sera for the respective study was approved by the Ethics committee of the Medical faculty of Heidelberg University (S-677/2020).

Serum Infection:

Huh7 Lunet C/M/S cells were seeded at a density of 2 or $1.5*10^4$ cells/well in 24 well plates the day before infection. Approximately 24 hours later, cells were inoculated with 80 µl patient serum mixed with 320 µl serum-free medium, and spin incubation was performed for 2 hours at 1000 g at RT. JC1cc administered with a MOI of 1 served as positive control. Samples were left at 37 °C for 2 to 3 h, next, the serum was removed and cells were incubated using complete DMEM supplemented with PI4KA/CKIa inhibitor treatment (PCi). According to the specific experiment, additional drugs (DCV, SIL, Alisporivir) were administered. In parallel, RNA from 200 µl serum was extracted using the NucleoSpin Virus kit (Macherey-Nagel) and analysed via RT-qPCR, to determine the viral load in copy number/mL of the patient serum. The samples were incubated for 72 h and harvested according to the respective readout, which consisted of either RT-qPCR or the newly established image-based analysis. For RT-qPCR, RNA extraction was performed using the NucleoSpin RNA Plus kit (Macherey Nagel) and the samples were then further processed using the BIO-RAD CFX Opus 96 Real-Time PCR System Thermal Cycler.

Automated Image Analysis (AIA):

For the image-based analysis, cells were fixed with 4% formaldehyde in PBS. After incubation at RT for 20 minutes, cells were washed 3 times with PBS. Next, cells were either stained with 4′,6-Diamidin-2-phenylindol (DAPI, Invitrogen) for 1 minute at a dilution of 1:4000 or stained with Hoechst 33342 (Sigma) for 5 minutes at a dilution of 1:2000 and then washed 3 times for 5 minutes. Images of the whole plates were taken using a Zeiss Cell Discoverer 7 microscope (CD7). Afterwards, the images were analysed via ilastik, an interactive learning and segmentation toolkit to detect co-localisation of the GFP and DAPI signal and hereby find and mark infected cells. To segment nuclei in stitched images we trained a Random Forest classifier based on the DAPI signal using ilastik [31]

Preprints.org (www.preprints.org) | NOT PEER-REVIEWED | Posted: 25 October 2024 doi:10.20944/preprints202410.2010.v1

which predicts semantic class attribution (nucleus or background) for every pixel. Objects obtained in this way were subsequently filtered by size to exclude unusually small or large nuclei which often represent aberrant biological structures or microscopy artefacts. Hysteresis algorithm was used to separate nuclei in close proximity to each other. In the next step, using ilastik object classification workflow, a machine learning algorithm was trained to classify objects into two categories—segmenting and classifying cells based on differences in GFP localization patterns between infected and not infected cells (ER localization = not infected, nuclear localization = infected).

The training set of data was arbitrary selected, and the same machine learning algorithm was used for the pixel and object classification in all images. Three training rounds were performed to reduce the background of false positive hits.

Cells marked as positive by the program were evaluated visually to reduce the false positive background to zero.

Pharmacological Inhibitors and Drugs:

The specific PI4KA inhibitor PI4KA-F1 was provided by Glaxo-Smith-Kline [32]; the CKIa-specific inhibitor H479 was a generous gift from Raffaele de Francesco (Milano, Italy) and has been described previously [23]. Legalon SIL was obtained from Madaus, Alisporivir from Debiopharm. The NS5A inhibitor Daclatasvir (DCV) was obtained from Bristol Myers Squibb.

Primers and Probes for RT-qPCR:

S_GAPDH (GAAGGTGAAGGTCGGAGTC); A_GAPDH (GAAGATGGTGATGGGATTTC); A_219_JFH (GGGCATAGAGTGGGTTTATCCA); S_146_JFH (TCTGCGGAACCGGTGAGTA); A165_Con1 (TACTCACCGGTTCCGCAGA); S59_Con1 (TGTCTTCACGCAGAAAGCGTCTAG)

GAPDH (6-VIC-CAAGCTTCCCGTTCTCAGCCT-TAMRA); CON1 (6-FAM-TCCTGGAGGCTGCACGACACTCAT-TAMRA); JFH (6-FAM-AAAGGACCCAGTCTTCCCGGCAATT-TAMRA)

Production of Viral Particles:

To produce JC1cc infectious particles, electroporation of in vitro transcribed JC1 RNA was performed and cells were incubated for 3 days. The medium was then filtered through a 0.45 µm filter and stored at 4 °C overnight. The cells were supplied with fresh DMEM. The next day, the DMEM was again removed and filtered. Filtered supernatant was concentrated using a Centricon Plus-70 centrifugal filter device (100 K nominal molecular weight limit; Merck) according to the manufacturer's instructions. Infectivity of the concentrated supernatant was determined via Tissue Culture Infectious Dose 50 (TCID50).

Cell Viability Assay:

Cells viability was measured using the Cell Titer Glo Luminescent Cell Viability Assay (Promega). Cells were seeded in 96 well plates with $1x10^4$ cells/well and incubated in complete DMEM supplemented with the various drug concentrations in triplicates. 3 wells were left empty for background control. After 3 days, the samples were measured according to the manufacturer's instructions using the Mithras LB 940 plate reader (Berthold Technologies). The results were analysed using Excel.

In Vitro Transcription, Electroporation and Luciferase Activity Assay:

In vitro transcription, electroporation and luciferase activity assay were performed as described previously [13]. Briefly 10 µg plasmid DNA were linearized with SpeI (Con1 and GLT1 based plasmids), MluI (JFH1 based plasmids) and XbaI (TN WT and DBN WT) and used as input for the in vitro transcription reaction. 2.5-5 µg purified HCV in vitro transcripts or the respective CN of patient derived RNA were electroporated into $2\text{-}4*10^6$ Huh7 Lunet C/M/S cells. Four hours after seeding the electroporated cells in 12 well dishes, drug treatments were performed. For luciferase activity assays,

Preprints.org (www.preprints.org) | NOT PEER-REVIEWED | Posted: 25 October 2024 doi:10.20944/preprints202410.2010.v1

cells were lysed at the respective time points and luciferase activity was measured using a Lumat LB9507 tube luminometer (Berthold Technologies). To account for variances in input RNA abundance, measured values were normalized to the luciferase activity at 4 h.

RT-qPCR:

RT-qPCR was performed measuring GAPDH-RNA as a control gene expressed ubiquitously in the host cells. A second primer set was used to detect HCV-RNA and was designed accordingly to the HCV genotype of the specific experiment. As a first step, a mastermix was prepared containing the two primer sets, two probes detecting GAPDH and HCV, the qScript XLT 1-step RT-PCT ToughMix (Quantabio) and distilled water to add up to the final volume. The mastermix was then pipetted into a 96 well PCR plate (hard-shell, thin-well, BioRad) using 12 µl per well. Next, a standard adjusted to the respective HCV genotype of the experiment was given to the first 24 wells ranging from $1x10^9$ to $1x10^2$ HCV-transcripts/µl. The samples for analysis (prepared from cells using the NucleoSpin RNA Plus kit by Macherey-Nagel) were pipetted into the remaining wells. 3 µl of standard/sample were used per well and measurements were done in triplicates. After preparation, the plate was sealed and analysed with the BIO-RAD CFX Opus 96 Real-Time PCR System Thermal Cycler using the "Taqman Quanta program" (Step 1: 50 °C for 10 min; Step 2: 95 °C for 1 min; Step 3: 95 °C for 10 secs; Step 4: 60 °C for 1 min; Repeat from Step 3 for 39 times). Results were exported to an Excel file and analysed there. If not stated otherwise, experiments were performed with three technical replicates per biological replicate.

Electroporation of HCV RNA from Patient Serum:

Viral RNA extracted from patient serum was electroporated into $2*10^6$ Huh7 Lunet C/M/S cells using a GenePulser system (BioRad) at 975 µF and 166 V in a cuvette with a gap width of 0.2 cm. Cells were then diluted in 8 mL DMEM and seeded into 12 well plates using 500 µl cell suspension and 500 µl fresh DMEM per well. PCi treatment was added to all samples, and as negative control, half of the wells were additionally treated with DCV. Samples were harvested after 72 hours and analyzed by RT-qPCR or by automated image analysis.

Liposome-Based Transfection:

The day before transfection, cells were seeded in 6 well plates using 2 to $2.5*10^5$ cells per well, leading to 80 to 90% confluence the next day. On the day of transfection, 3.75 µl of Lipofectamine MessengerMax (Thermo Fisher) reagent were mixed with 125 µl OptiMEM (Gibco) and incubated for 15 minutes at RT. The RNA for transfection was given into 125 µl OptiMEM as well, the two tubes were combined and then incubated for 5 minutes. The 250 µl end product were pipetted onto the 6 well plate, which had been preincubated with OptiMEM at 37 °C for approximately 30 minutes. After 4 hours, OptiMEM was removed and substituted by complete DMEM. The next day, the cells were split according to the respective experiment.

Ultracentrifugation:

To prepare a sucrose cushion, 20% sucrose were dissolved in TNE buffer, filtered sterilely, and stored at 5 °C. To concentrate viral RNA from patient serum, 2.5 mL sucrose in TNE buffer were overlaid with 10 mL patient serum mixed with 20 mL PBS in an ultracentrifugation tube. Ultracentrifugation was performed at 28000 rounds per minute (rpm) and 4 °C for 2 hours using a Beckmann rotor SW32. Afterwards, centrifuge tubes were emptied and dried, leaving a pellet containing the viral particles. The pellet was dissolved in 750 µl TRIzol (Ambion) and RNA extraction was performed according to the standard protocol.

TRIzol LS Extraction:

For TRIzol LS extraction, 200 µl of serum were mixed with 600 µl TRIzol LS reagent and incubated for 5 minutes at RT. Then, 160 µl chloroform were added and the mixture was shaken

Preprints.org (www.preprints.org) | NOT PEER-REVIEWED | Posted: 25 October 2024 doi:10.20944/preprints202410.2010.v1

vigorously by hand for 15 seconds. After incubation at RT for 2-3 minutes, centrifugation at 12,000 g for 15 minutes at 4 °C was performed to achieve phase separation. The upper phase was transferred into a new tube, mixed with 400 µl isopropanol and incubated at RT for 10 minutes. Next, the mixture was centrifuged at 12,000 g for 10 minutes at 4 °C and afterwards the supernatant was removed, leaving the RNA pellet. 1 mL 75% ethanol was added, and the sample was centrifuged at 7500 g for 5 minutes at 4 °C. The ethanol was removed, the pellet was air-dried for 5 minutes and afterwards resuspended in 30 µl dH_20. The sample was incubated at 55-60 °C on a heat block, and then stored at -80 °C.

Statistical Analysis:

Statistical analysis was performed in Graph Pad Prism using the unpaired Student's t-test.

Results

Establishment of Optimal Conditions for Serum Infection

In this study, we aimed at establishing a cell culture model for robust detection of serum derived HCV infection. To this end, we used Huh7-Lunet CD81H/MAVS-GFP-NLS/SEC14L2 cells (Huh7-Lunet C/M/S) stably expressing three transgenes: CD81, a crucial entry receptor, which is not efficiently expressed in Huh7-Lunet cells [33]; SEC14L2, facilitating RNA replication of HCV WT isolates [25] and GFP fused to a nuclear localization signal (GFP-NLS) and the C-terminus of MAVS including the NS3-4A cleavage site, allowing the detection of HCV infection by nuclear transfer of GFP-NLS [21,34]. We had previously identified a SEC14L2 independent strategy to promote RNA replication of HCV gt1b WT isolates based on combined inhibition of PI4KA/CKIa (PCi treatment) [21]. Since we found some additive effect upon combination of PCi and SEC14L2 [24], we first aimed to optimize PCi concentrations in Huh7-Lunet C/M/S, using subgenomic reporter replicons. We used two gt1b WT genomes with variable replication capacity, Con1 and GLT1 [24], since this genotype has been shown to be most efficiently stimulated by SEC14L2 [25,26] and PCi treatment [21]. Using a fixed concentration of 5 µM of the CKIa-inhibitor H479, we tested variable concentrations of the PI4KA-inhibitor F1 (Figure 1A). A moderate enhancement of replication for both isolates could be detected up to a concentration of 10 nM followed by a decline at higher concentrations, similar to our previous results [21]. The combination of 5 µM H479 and 5 nM F1 was chosen for all later experiments.

We next titrated the NS5A-inhibitor Daclatasvir (DCV), which we planned to use as a control to define active replication in the infection assay. Already at 0.1 nM, replication of both isolates was suppressed to the level of a replication deficient control (ΔGDD, Figure 1B). Since no cytotoxicity was observed at any concentration (Figure 1C), we chose 1 nM DCV for further experiments, to inhibit also WT isolates with potentially lower DCV sensitivity.

To explore the dynamic range of various detection methods in greater detail, we included two additional antiviral agents, namely Legalon SIL (SIL) and Alisporivir (Alis), both being potential candidates for patients failing to be cured by current DAA regimens [35]. Legalon SIL exhibited antiviral effects against HCV in some patients [36], with a yet poorly understood selectivity towards certain isolates and genotypes [37]. Alisporivir is a non-immunosuppressive Cyclophilin A inhibitor blocking efficiently the interaction with NS5A [38–40]. Both compounds were tested in Huh7 Lunet C/M/S cells with the same experimental set up as used for DCV. The Con1 WT replicon was entirely inhibited by SIL concentrations above 250 µM (Figure 1D). For GLT1, a drop in replication was observed as well, but levels stayed clearly above the negative control hinting to a partial resistance, as observed before for other HCV isolates like JFH1 [37]. Due to inhibitory effects on cell growth upon rising concentrations (Figure 1E), 250 µM was chosen as a standard concentration. Also, in case of Alisporivir GLT1 was less sensitive than Con1, requiring 1 µM Alisporivir for complete inhibition (Figure 1F). This concentration was used in subsequent experiments since it further lacked cytotoxic effects (Figure 1G).

Preprints.org (www.preprints.org) | NOT PEER-REVIEWED | Posted: 25 October 2024 doi:10.20944/preprints202410.2010.v1

All data generated so far were based on luciferase activity measurement upon transfection of reporter replicons. However, RT-qPCR was one method of choice to measure HCV replication upon infection with HCV positive sera. We therefore aimed to define the dynamic range of the two assays, using DCV, Legalon-SIL and Alisporivir. We chose cell lines harbouring persistent, selectable reporter replicons, since electroporation of in vitro transcribed viral genomes would have generated a high background in RT-qPCR. To that end, we used already established cell lines based on Con1 [27], JFH1 [28] and a newly generated a cell line containing GLT1 WT. All three cell lines were treated with the previously determined standard concentrations of SIL, Alisporivir or DCV, harvested after 24, 48 and 72 h and analysed for luciferase activity (Figure 2A, upper panels) or by RT-qPCR (Figure 2A, lower panels). In principle, we observed the same pattern of sensitivity to the different drugs in both assays for all three replicons, with Con1 being highly sensitive to all compounds, whereas GLT1 was less sensitive and JFH1 completely resistant to Legalon-SIL. However, while the reporter assay offered a reduction upon full inhibition of more than two logs, the dynamic window of the RT-qPCR assay was much lower, as expected [28].

Finally, we validated our model in infection, using JC1cc and GLT1 patient serum as positive controls, the latter had already shown robust cell culture replication upon PCi-treatment in a previous study [21] (Figure 2B). JC1cc RNA levels were reduced by more than two logs upon Alisporivir and DCV treatment and not affected by Legalon-SIL, comparable to the results obtained with the replicon cells (Figure 2A, right panels). In case of GLT1 serum infection, no pronounced additive effect of the combination of PCi treatment and SEC14L2 overexpression in comparison to PCi treatment alone could be detected when compared to the earlier results [21]. This was also in line with previous observations using the GLT1 replicon ([24] and Figure 1A). The drug treatments clearly reduced HCV RNA levels, indicating a successful infection followed by viral replication. However, the reduction compared to the untreated control was only fivefold. The much smaller window between infection and DCV treated samples in comparison to the JC1cc control could be due to the difference in replication efficiency in cell culture, which is exceptionally high for JC1. It could further point to a larger impact of remaining input RNA when working with patient sera, e.g. due to a higher number of defective particles attaching to, but not entering the cells. However, the level of reduction detected by RT-qPCR did not reach statistical significance. Of note, the GLT1 patient serum appeared to be more sensitive to SIL treatment than the GLT1 WT subgenomic replicon. This could be explained by SIL acting on multiple steps of the HCV life cycle [41,42] including steps like cell entry which are relevant during serum infection but not in subgenomic replicons [43].

Overall, we optimized a cell culture model based on Huh7-Lunet C/M/S cells by combining SEC14L2 expression and PCi treatment, principally allowing the analysis of HCV infection using patient sera. However, the dynamic range obtained by RT-qPCR was relatively low, even in case of a high-titer post-transplant serum.

Preprints.org (www.preprints.org) | NOT PEER-REVIEWED | Posted: 25 October 2024 doi:10.20944/preprints202410.2010.v1

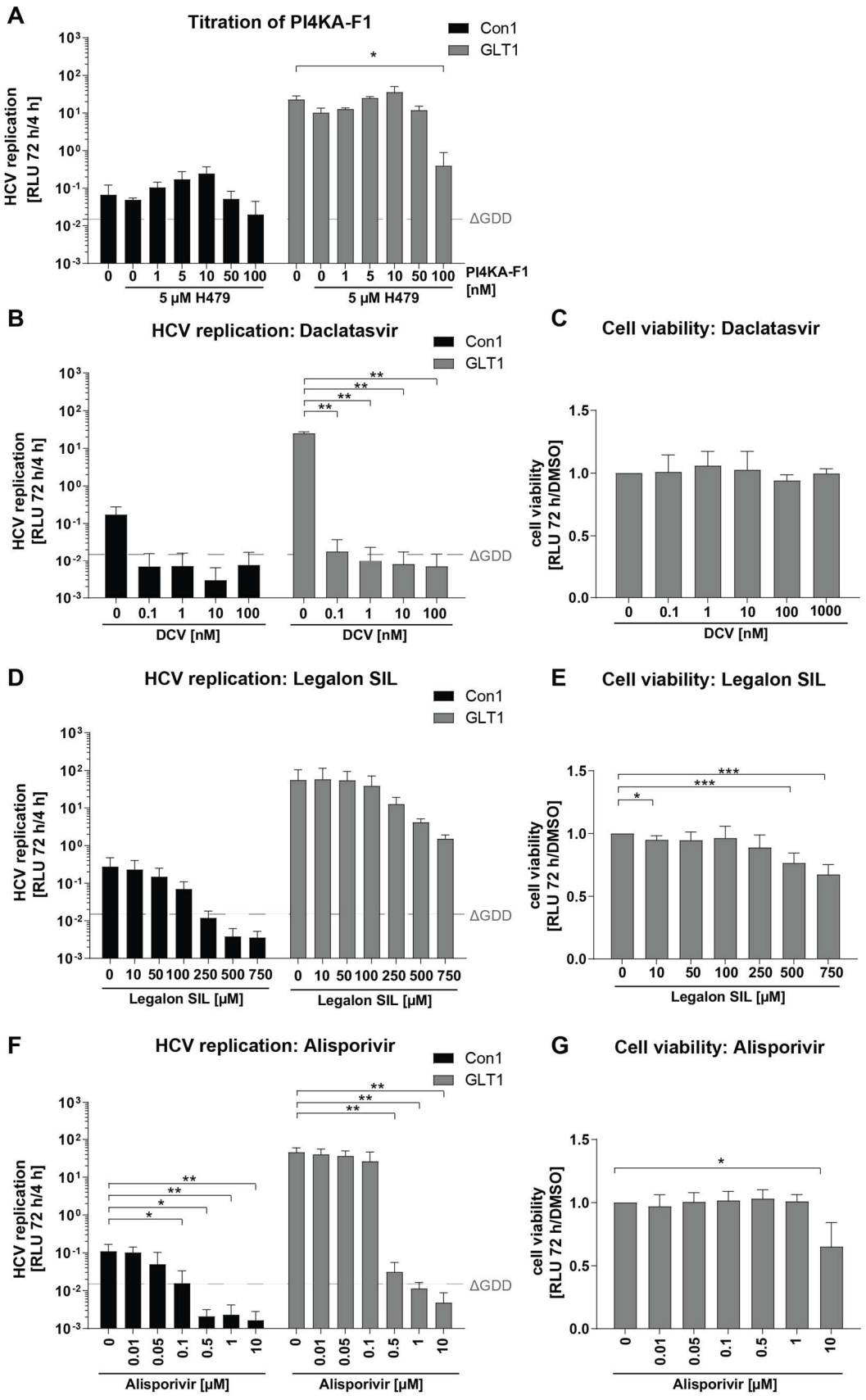

Figure 1. Establishment of a cell culture model to assess HCV WT replication. (A, B, D, F) Subgenomic reporter replicons based on Con1 WT and GLT1 WT were electroporated into Huh7-Lunet C/M/S cells and treated with either DMSO or the indicated concentrations of (A) H479 combined with PI4KA-F1 (PCi), or with PCi and the indicated concentrations of DCV (B)/Legalon SIL

Preprints.org (www.preprints.org) | NOT PEER-REVIEWED | Posted: 25 October 2024 doi:10.20944/preprints202410.2010.v1

(D)/Alisporivir (F) at 4 h after electroporation. Cells were harvested 72 h later and firefly luciferase activity from cell lysates (RLU) was quantified as a correlate of RNA replication efficiency and normalized to 4 h. A replication deficient Con1 variant (ΔGDD) served as negative control and is indicated with a dashed grey line. Values are shown as means from two (A, B) or three (D, F) independent experiments with two technical replicates each. (C, E, G) Huh7-Lunet C/M/S cells were seeded into 96 well plates and treated with the indicated concentrations of DCV (C)/Legalon SIL (E) or Alisporivir (G). After 72 h, cell viability in cell lysates was measured Cell-titer-Glow and normalized to the DMSO control. Values are shown as means from at least three independent experiments. *P < 0.05, **P < 0.01, ***P < 0.001 (unpaired two-tailed Student's t-test).

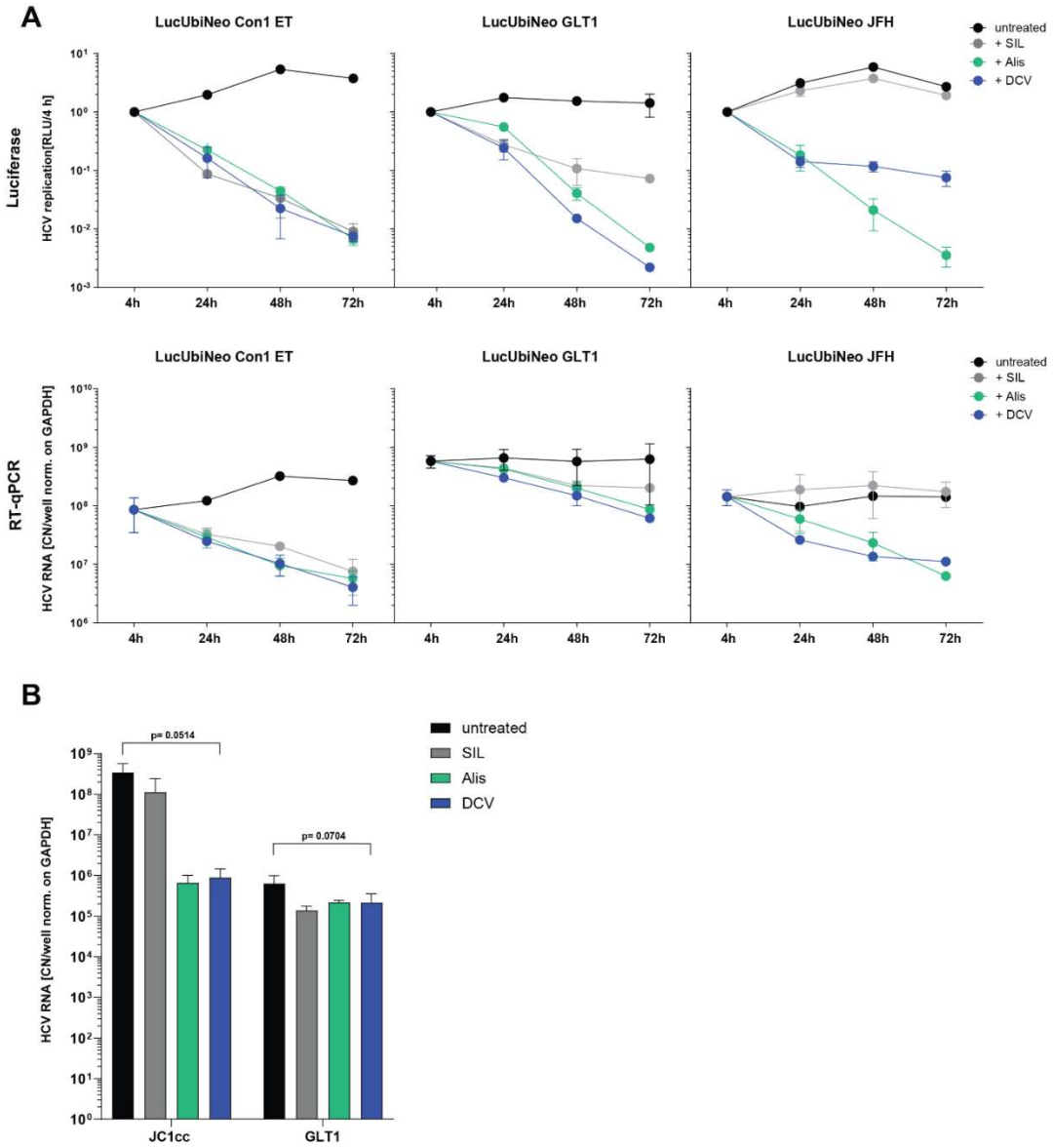

Figure 2. Comparison of luciferase activity and RT-qPCR based readouts in persistent replicon cells and HCV infected cells. (A) Cell lines harbouring the indicated replicons were treated with 250 µM SIL, 1 µM Alisporivir, 1 nM DCV or were left untreated, and harvested at the indicated time points. Upper panels: Firefly luciferase activity from cell lysates (RLU) was quantified as a correlate of RNA replication efficiency and is normalized to 4 h. Values are shown as means from two independent experiments with two technical replicates each. Lower panels: After RNA extraction, HCV RNA copies were quantified using RT-qPCR. HCV RNA copy numbers (CN) were normalized on GAPDH and are shown as CN per well. Values are shown as means from two independent experiments with three technical replicates each. (B) Huh7-Lunet C/M/S cells were infected with either GLT1 patient serum or JC1 infectious particles (MOI of 10 at the first repetition, MOI of 1 at the second

Preprints.org (www.preprints.org) | NOT PEER-REVIEWED | Posted: 25 October 2024 doi:10.20944/preprints202410.2010.v1

and third repetition). After 72 hours, samples were harvested and HCV RNA replication was measured via RT-qPCR. HCV RNA copy numbers (CN) were normalized on GAPDH and are shown as CN per well. Values are shown as means of four (GLT1: untr. + DCV), three (JC1: untr. + DCV), or two (GLT1 and JC1: SIL and Alisporivir treatment) independent experiments with three technical replicates each. P-values from unpaired two-tailed Student's t-test are indicated.

Establishment of a Quantitative, Semi-Automated Image Analysis Pipeline for Serum Infection

We then started testing a first cohort of 27 HCV positive patient sera, mainly gt1b, based on a previously established serum infection protocol [21] (Figure 3A, Table 3). DCV treatment was included to define bona fide viral replication from viral input RNA. We additionally determined the viral RNA titer of all sera, using the same RT-qPCR assay as for the quantification of viral replication after infection (Table 3). Unfortunately, HCV RNA was clearly detectable post infection (Ct<36) only for the two sera with highest titers (Table 3) and no infection showed a significant reduction upon DCV treatment (not shown). We therefore decided to establish an image-based readout utilizing the GFP reporter system contained in the Huh7-Lunet C/M/S cells [34]. Due to our previous experience, suggesting an overall very low number of infection events [21], we aimed at imaging whole wells and implementing an automated readout to generate accurate and reproducible results. To that end, a Zeiss Cell Discoverer 7 microscope (CD7) was used combined with automated image analysis by ilastik [31], a machine-learning image analysis tool, segmenting and classifying cells based on differences in GFP localization patterns between infected and not infected cells (ER localization = not infected, nuclear localization = infected) (Figure 3B). Ilastik was trained with images of cells infected with JC1cc using DCV treatment and uninfected cells as negative controls, resulting in a robust, significant detection of infected cells (Figure 3C). After three iterative training sets, the background of false positive detections could be reduced from 2% to 0.01-0.02% (Figure 3D), corresponding to about 100 cells in a 24 well dish. However these low background levels still surpassed the true positive hits, so AIA had to be followed by visual validation of the annotated positive hits. Nevertheless, this still was a major gain in efficiency, since only 100 instead of ~300,000 to 500,000 cells had to be visually inspected. Visual validation of hits automatically assigned by ilastik revealed not a single truly positive cell in any of the JC1cc infected samples with DCV treatment or in the negative controls, arguing for the stringency of this analysis pipeline. The automated image analysis (AIA) followed by a visual validation thereby allowed quantification of infected cells in absence of any false positive signals (Figure 3E).

Table 3. Sera used for RT-qPCR analysis only.

Serum	Date and cohort	Titer[1]	Gt	HCV RNA pi[2]
4468	2016 Frankfurt 2016(DZIF)2016	1,02E+07	1b	Yes
5342	2016 Frankfurt	5,78E+05	1b	No
3617	2015 Frankfurt	3,81E+06	1b	Cells died
2054	2015 Frankfurt	4,10E+05	1b	No
4695	2016 Frankfurt	2,97E+05	1b	No
2823	2021 Frankfurt	9,73E+05	1b	No
3260	2015 Frankfurt	1,95E+06	1b	No
7437	2016 Frankfurt	3,07E+05	1b	No
5120	2016 Frankfurt	7,64E+05	1b	No
4153	2016 Frankfurt	7,61E+05	1b	No
4886	2016 Frankfurt	4,98E+05	1b	No
3676	2015 Frankfurt	2,00E+06	1b	No
6936	2017 Frankfurt	6,52E+05	1b	No
6087	2017 Frankfurt	2,90E+05	1b	No
4202	2016 Frankfurt	1,72E+04	1b	No

Preprints.org (www.preprints.org) | NOT PEER-REVIEWED | Posted: 25 October 2024 doi:10.20944/preprints202410.2010.v1

5613	2017 Frankfurt	1,89E+05	1b	No
1199	2014 Frankfurt	7,24E+03	1b	No
1597	2015 Frankfurt	3,01E+06	1b	Cells died
521	2020 Heidelberg	7,85E+05	1a	No
566	2020 Heidelberg	Not detectable	1b	No
574	2020 Heidelberg	2,72E+06	1b	No
572	2020 Heidelberg	4,24E+05	1b	No
77	2013 Heidelberg	3,92E+03	1b	No
570	2020 Heidelberg	2,98E+05	1b	No
579	2020 Heidelberg	8,96E+03	1a	No
210	2014 Frankfurt (DZIF)	1,78E+06	1b	No
GLT1	2014 Heidelberg	4,22E+07	1b	Yes

[1][RNA copies/mL] [2]CT<36.

Preprints.org (www.preprints.org) | NOT PEER-REVIEWED | Posted: 25 October 2024 doi:10.20944/preprints202410.2010.v1

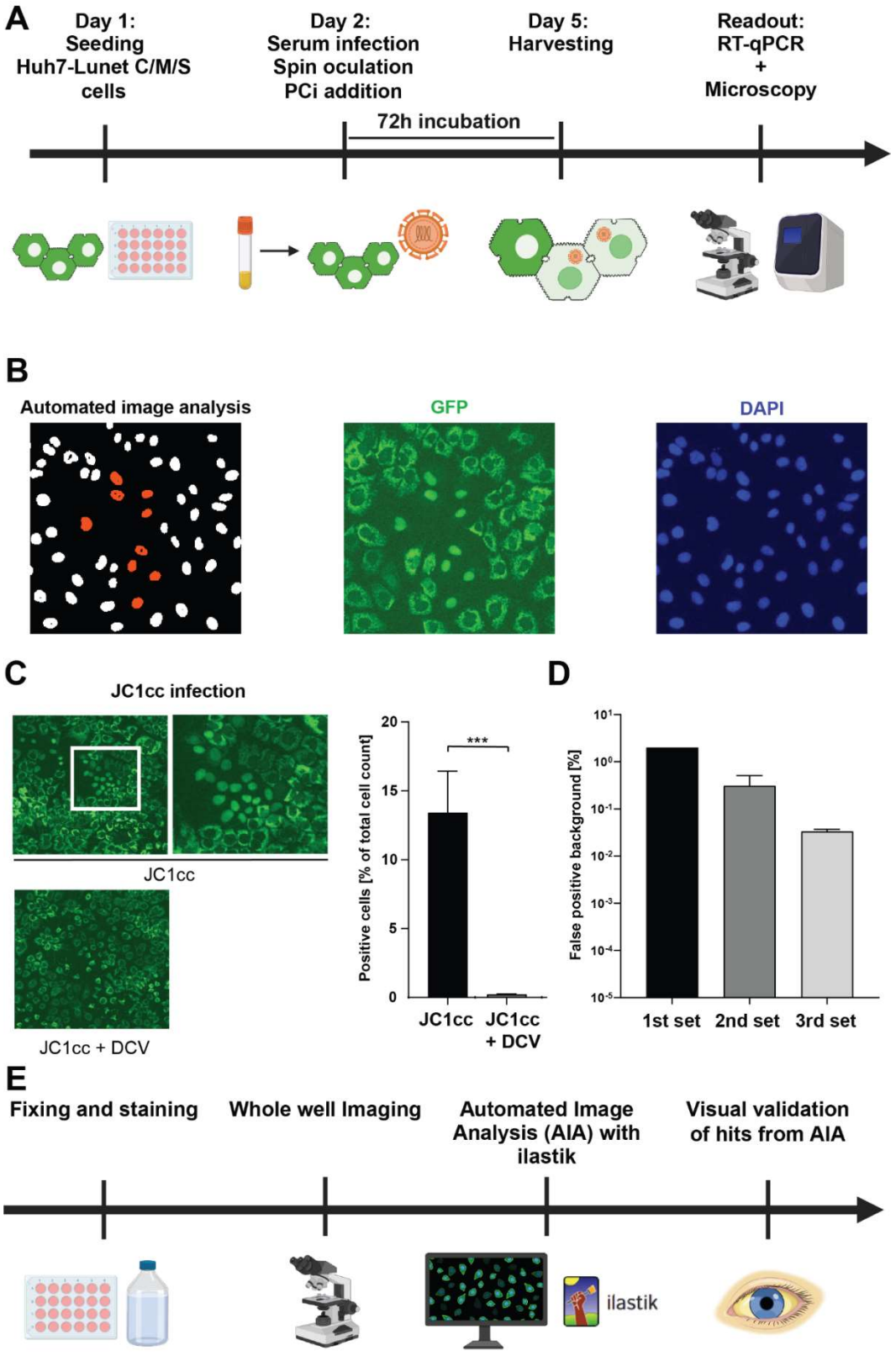

Figure 3. Workflow for serum infection and establishment of semi-automated image analysis. (A) Workflow for serum infection. (B) Principle of automated image analysis by machine learning. Infected cells are identified by nuclear GFP due to co-localization with DAPI. Positive cells were marked in red by ilastic, facilitating visual validation. (C) Huh7-Lunet C/M/S cells were infected with JC1cc (MOI=1) alone or additionally treated with DCV, fixed and stained with DAPI 72 h post infection. A group of infected cells is indicated by a white box and additionally displayed with a higher magnification. Percentage of positive cells (right panel) was obtained by automated image analysis. (D) Optimization of the automated image analysis. False positive background in images of

Preprints.org (www.preprints.org) | NOT PEER-REVIEWED | Posted: 25 October 2024 doi:10.20944/preprints202410.2010.v1

either uninfected or DCV treated cells was reduced by iterative training of the machine learning tool, including adjustment of cell count per well and refocusing strategy. (E) Workflow of automated image analysis (AIA) followed by visual validation.

Semi-Automated Image Analysis Revealed More Consistent Results upon Serum Infection than RT-qPCR

We next aimed to analyse whether semi-automated image analysis enabled a thorough determination and quantification of infections using HCV WT isolates from serum. Based on the previous experience, samples with high viral loads of $>10^6$ RNA copies per mL were chosen for further infection experiments to compare RT-qPCR and image analysis (Table 1). 11 out of 29 gt1b sera were taken after liver transplantation, including GLT1, providing a better chance of success due to high viral loads and the potential lack of neutralizing antibodies. The limited amount of available sera (1 mL or below), allowed for triplicate infections for both methods, including the DCV controls.

HCV RNA was detectable by RT-qPCR in 11 infections, however, a statistically significant drop in RNA copy numbers upon DCV treatment was only found in 1 case (serum 81) and more than 2fold reductions lacking significance in an additional 2 cases (GLT1 and serum 2130, Figure 4A, Table 1). The fully automated image-based analysis revealed a slightly varying background of 0.02-0.07%, judged by the DCV controls, due to disruptive factors like locally increased cell density or ill-focused images. Statistically significant reductions upon DCV treatment were obtained only for three sera, 60, 84 and GLT1 (Figure 4B), suggesting that the number of positive cells was below the background of false positive detections in most cases. In contrast, the automated analysis combined with visual validation identified infected cells with verified *bona fide* nuclear GFP signal in overall 11 cases, ranging from a total number of 1 to about 200 infected cells per well (Figure 4C, Table 1). All sera showing clearly detectable or significant differences in the RT-qPCR analysis (Figure 4A) or the automated image analysis (Figure 4B), respectively, indeed were verified to contain infected cells. In case of serum 14 and 5651, only a single infected cell was detected in one or two wells, respectively. Importantly, again not a single positive cell with nuclear GFP was found in any of the DCV treated controls. Overall, the automated image analysis combined with visual validation offered a highly sensitive proof of successful infection due to the lack of any background thereby allowing to identify even a single infected cell, in contrast to genome detection by RT-qPCR.

We next analysed, whether the titer and the transplant status of the tested patient sera did have an impact on the respective success of a serum infection (Figure 4D). Indeed, we found a significant correlation between serum RNA titer and successful detection of infection events. All sera with titers above $1*10^7$ RNA copies/mL resulted in detectable infected cells, but based on the limited data, we could not define a lower threshold. Post-transplant sera had a higher success rate (8/11 gt1b sera compared to 7/23 non-transplant sera), but also had on average higher titers.

Taken together, we were able to establish a robust infection model for HCV patient sera, based on a semi-automated image analysis pipeline using Huh7-Lunet C/M/S cells.

Table 1. Sera used for comparative analysis of RT-qPCR and Automated Image Analysis (AIA).

Serum	Date and cohort	Titer[1]	LTx[2] y/n	Gt	HCV RNA pi[3]	Infected cells[4]	Difference to DCV control p<0.05 (RT-qPCR / AIA)
1aHT	2016 Heidelberg	4,25E+06	y	1a	No	No	No / No
1	2010 Barcelona	3,24E+07	y	1b	Yes	Yes	No / No
14	2011 Barcelona	6,74E+06	y	1b	Yes	Yes	No / No
41	2012 Barcelona	8,74E+06	y	1b	Yes	Yes	No / No
43	2012 Barcelona	3,84E+06	y	1b	Yes	Yes	No / No
44	2012 Barcelona	9,11E+06	y	1b	Yes	No	No / No
60	2012 Barcelona	5,04E+07	y	1b	Yes	Yes	No / Yes
76	2013 Barcelona	4,95E+06	y	1b	Yes	No	No / No

Preprints.org (www.preprints.org) | NOT PEER-REVIEWED | Posted: 25 October 2024 doi:10.20944/preprints202410.2010.v1

81	2014 Barcelona	1,03E+07	y	1b	Yes	Yes	Yes / No
84	2014 Barcelona	1,24E+08	y	1b	Yes	Yes	No / Yes
88	2014 Barcelona	1,13E+06	y	1b	No	No	No / No
1673	2015 Frankfurt	9,88E+05	n	1b	No	No	No / No
1730	2015 Frankfurt	1,49E+06	n	1b	No	No	No / No
1754	2015 Frankfurt	1,68E+06	n	1b	No	No	No / No
2014	2015 Frankfurt	1,79E+06	n	1b	No	No	No / No
2072	2015 Frankfurt	2,35E+06	n	1b	No	No	No / No
2121	2015 Frankfurt	2,87E+06	n	1b	No	No	No / No
2130	2015 Frankfurt	4,97E+06	n	1b	Yes	Yes	No / No
2149	2015 Frankfurt	2,11E+06	n	1b	No	Yes	No / No
2213	2015 Frankfurt	1,29E+06	n	1b	No	No	No / No
2282	2015 Frankfurt	2,02E+06	n	1b	No	No	No / No
2289	2015 Frankfurt	1,46E+06	n	1b	No	No	No / No
2668	2015 Frankfurt	2,46E+06	n	1b	No	No	No / No
2672	2015 Frankfurt	2,55E+06	n	1b	No	No	No / No
2711	2015 Frankfurt	2,17E+06	n	1b	No	No	No / No
3266	2015 Frankfurt	2,37E+06	n	1b	No	No	No / No
4244	2015 Frankfurt	3,06E+06	n	1b	No	No	No / No
5651	2016 Frankfurt	2,17E+06	n	1b	No	Yes	No / No
GLT1	2014 Heidelberg	4,22E+07	y	1b	Yes	Yes	No / Yes

[1][RNA copies/mL] [2]Serum post LTx [3]CT<36 [4]Automated image analysis (AIA) verified by visual control.

Preprints.org (www.preprints.org) | NOT PEER-REVIEWED | Posted: 25 October 2024 doi:10.20944/preprints202410.2010.v1

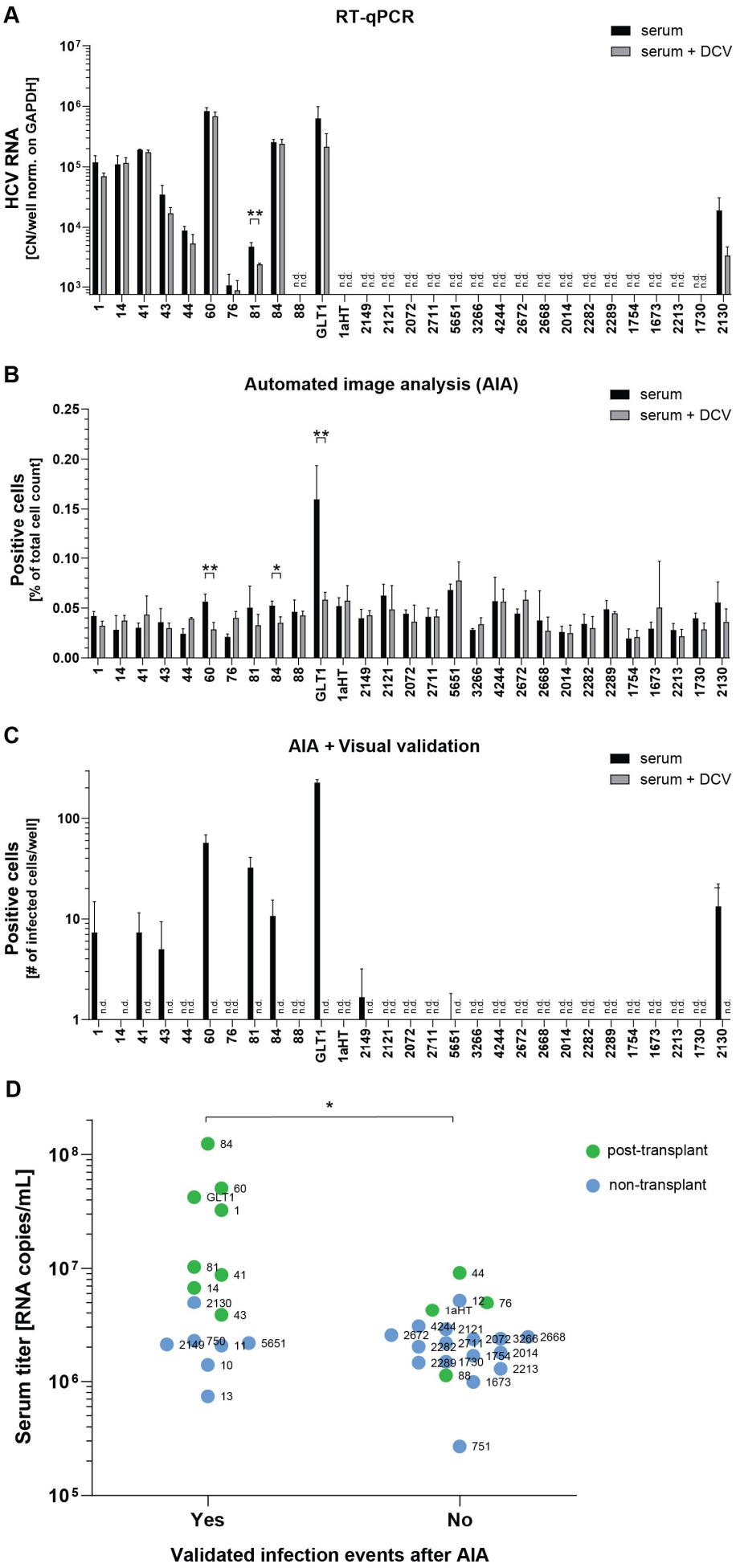

Preprints.org (www.preprints.org) | NOT PEER-REVIEWED | Posted: 25 October 2024 doi:10.20944/preprints202410.2010.v1

Figure 4. Comparison of HCV infection using high-titer sera by RT-qPCR or microscopic analysis. (A-C) Huh7-Lunet C/M/S cells treated with PCi and infected with patient sera in presence or absence of DCV. 72 h after infections, cells were fixed, stained with DAPI. (A) Total RNA was extracted 72 h after infection and HCV RNA was quantified. (B) 72 h after infections quantification by automated image analysis was performed. (C) Truly infected cells detected after visual validation of hits generated by the automated image analysis. Note that no *bona fide* infected cells were detected in the DCV treated samples. All values are means and SD of three or two (serum 44) independent biological replicates. Note that RT-qPCR data from the GLT1 serum was taken from Figure 2B to allow a direct comparison (n=4). n.d.: not detectable. *P < 0.05, **P < 0.01 (unpaired two-tailed Student's t-test). (D) Results of the semi-automated image based analysis of all data shown in panel C and in Figure 6C were analysed regarding the impact of RNA titer and post-transplant status on infection outcome. The anonymised abbreviation of each serum is given next to the respective dot (see Tables 1 and 2). Samples were judged positive if at least one infected cell was found via the automated image analysis combined with visual validation. *P < 0.05 (unpaired two-tailed Student's t-test).

Table 2. Patient Sera used for electroporation (epo) after RNA extraction.

Serum	Date of aquisition	Serum titer[1]	Gt	LTx[2] y/n	Serum volume	Input infection[3]	Input epo[3]
10	2015 Freiburg	1,40E+06	1b	n	10 mL*	1,12E+05	9,06E+05
11	2015 Freiburg	2,07E+06	1b	n	10 mL*	1,66E+05	4,89E+05
12	2015 Freiburg	5,20E+06	1b	n	10 mL*	4,16E+05	5,67E+06
13	2015 Freiburg	7,41E+05	1b	n	10 mL*	5,93E+04	1,02E+06
750	2022 Heidelberg	2,28E+06	1b	n	10 mL*	1,82E+05	2,70E+04
751	2022 Heidelberg	2,69E+05	1b	n	10 mL*	2,15E+04	2,10E+04
2130	2015 Frankfurt	4,97E+06	1b	n	1 mL	3,98E+05	1,06E+06
2213	2015 Frankfurt	1,29E+06	1b	n	1 mL	1,03E+05	7,31E+05
GLT1	2014 Heidelberg	4,22E+07	1b	y	1 mL	3,38E+06	1,22E+06
1aHT	2016 Heidelberg	4,25E+06	1a	y	1 mL	3,40E+05	6,19E+04

[1][RNA copies/mL] [2]Serum post LTx [3][RNA copies] per well *known storage history, no freeze/thaw cycles.

Establishment of Transfection-Based Delivery of Serum-Derived HCV WT RNA

Since titers above 10^6 RNA copies/mL are rare, and the infectious capacity of the serum samples might have been affected by multiple factors such as neutralizing antibodies, damaged infectious particles, cytotoxicity of some serum components and many more, we tested whether transfection of viral RNA extracted from serum samples would lead to more effective HCV WT replication in Huh7-Lunet C/M/S cells. Such an approach would further allow upscaling by using a higher volume of serum for RNA extraction. As a first step, a transfection protocol was established comparing lipid-based transfection and electroporation of in vitro transcribed HCV WT RNA (Figure 5). To that end, full length in vitro transcripts of the GLT1 WT consensus sequence, the gt1a isolate TN WT [19] and the gt3a isolate DBN WT [20] were used in increasing concentrations. Measurable HCV RNA levels in RT-qPCR could reliably be observed starting from an RNA copy number of 10^8 with both methods, lipid-based transfection and electroporation (Figure 5A, B). This was the case for all three isolates independently of the genotype. However, when compared to the DCV control, only the GLT1 isolate exhibited a reproducible reduction in HCV copy numbers under all conditions, suggesting that gt1a and gt3a WT replication was not supported to the same extent as gt1b upon SEC14L2 expression and PCi treatment, in line with previous studies [21,26]. Interestingly, DCV resulted in a far stronger decrease in the RNA signal after electroporation, suggesting that naked viral input RNA might be degraded more efficiently than in vitro transcripts complexed in transfection reagents, resulting in lower background.

In the automated image analysis, a rise in positive cell numbers compared to DCV using the GLT1 isolate could be detected starting from 10^9 RNA copies upon electroporation and 10^{10} RNA copies upon lipid-based transfection. Using the visual validation, a few cells with nuclear GFP signal

Preprints.org (www.preprints.org) | NOT PEER-REVIEWED | Posted: 25 October 2024 doi:10.20944/preprints202410.2010.v1

were already found in samples transfected with 10^7 RNA copies upon electroporation (Figure 5C) and 10^8 copies upon lipid-based transfection (Figure 5D). Again, no validated positive cells were found after DCV upon electroporation (data not shown), suggesting that translation of NS3-4A from transfected input RNA was not sufficient to confer nuclear GFP translocation. In contrast, a high number of positive cells were detected in the DCV treated control after lipid-based transfection, starting from 10^9 RNA copies, because DCV was added only 24 hours after addition of the transfection mixture, after splitting of the cells, to avoid interference of both treatments. In line with previous studies, this was obviously too late to impede nuclear GFP translocation [24,34,44]. TN WT and DBN3a WT did not show a significant rise in positive cells with both transfection methods, even when high amounts of input RNA were used. Upon visual validation, a few infected cells were detected with an input of 10^{10} RNA copies for both isolates and transfection methods. Therefore, also non gt1b isolates appeared to be able to replicate in this assay, although to a much lower extent.

Overall, electroporation was chosen for further studies, since positive cells could already be detected at lower input RNA copy numbers and due to lower background in RT-qPCR.

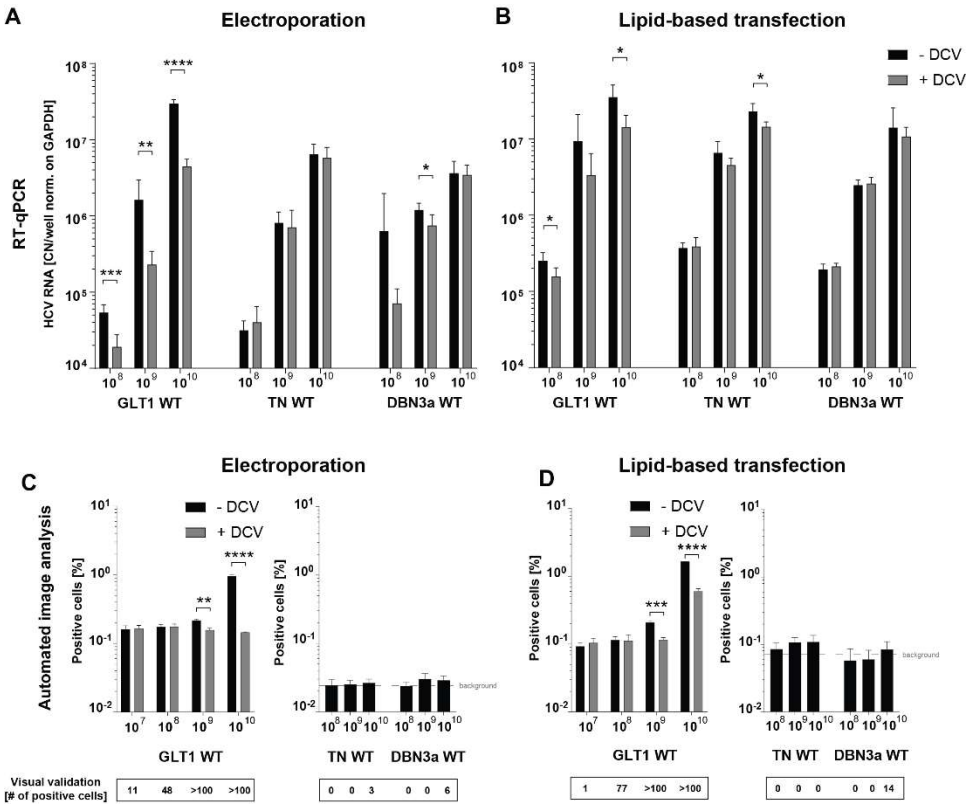

Figure 5. Establishment of an HCV WT RNA transfection protocol. In vitro transcribed RNA of GLT1 WT (gt1b), TN WT (gt1a) and DBN WT (gt3a) was transfected into Huh7 Lunet C/M/S cells with different amounts of input RNA, ranging from 10^7 to 10^{10} RNA copies per transfection, either by electroporation (A, C) or by lipid-based transfection (B,D). RT-qPCR (A, B) and the automated image analysis served as readout (C, D). Samples were measured in technical triplicates. In the image-based analysis (C,D), the samples transfected with 10^8 RNA copies of TN WT and DBN WT were set as false positive background, since no infected cells could be detected upon visual validation, depicted as a dashed grey line. Numbers of cells visually validated represent only DCV- samples. (A, C) Electroporation: Samples were harvested after 72 hours. Values are taken from two (TN WT, DBN WT) or three (GLT1 WT) independent experiments. (B, D) Lipid-based transfection: Cells were split 24 h post transfection, at this time point DCV was added. Samples were harvested after 2 (to stick to the total incubation time of 72 h) or 3 (to ensure DCV treatment for 72 h) days. Since there were no relevant differences in the results with varying incubation times observed, the data of the two experiments is shown in the same graph. *P < 0.05, **P < 0.01, ***P < 0.001, ****P < 0.0001 (unpaired two-tailed Student's t-test).

Preprints.org (www.preprints.org) | NOT PEER-REVIEWED | Posted: 25 October 2024 doi:10.20944/preprints202410.2010.v1

We used 10 patient sera to compare infection with transfection of viral RNA (Figure 6). For 4 sera RNA was extracted from 1 mL volume using TRIzol LS, for 6 serum samples we first aimed to concentrate virus from approximately 10 mL serum by ultracentrifugation prior to RNA extraction. However, ultracentrifugation from larger volumes did not necessarily result in increased viral RNA yields, indicating that a substantial amount of viral RNA was lost (Table 2). Transfection and infection were compared by RT-qPCR and by image analysis.

For transfection of RNA derived from serum 2130, we obtained a significant increase in viral RNA and a substantial number of positive cells upon AIA with visual validation (Figure 6A, C), providing proof of concept that transfection of serum derived viral RNA indeed is a feasible approach to study replication of WT isolates in cell culture. However, no significance was reached with AIA, due to variable seeding densities after electroporation, resulting in high background (Figure 6B) and only two additional transfected RNAs yielded single positive cells (Figure 6C, left panel). The same set of samples were positive upon infection plus an additional 4 sera which were negative upon transfection (Figure 6C, right panel). The reason for failure of RNA extracted from GLT1 to mount replication upon transfection despite efficient RNA extraction was not clear.

Overall, transfection of viral RNA extracted from serum so far provided no benefit compared to infection, albeit possible in principle. A thorough optimization of enrichment of viral RNA from larger serum volumes still holds the promise to widen the scope of sera applicable for testing in cell culture.

Preprints.org (www.preprints.org) | NOT PEER-REVIEWED | Posted: 25 October 2024 doi:10.20944/preprints202410.2010.v1

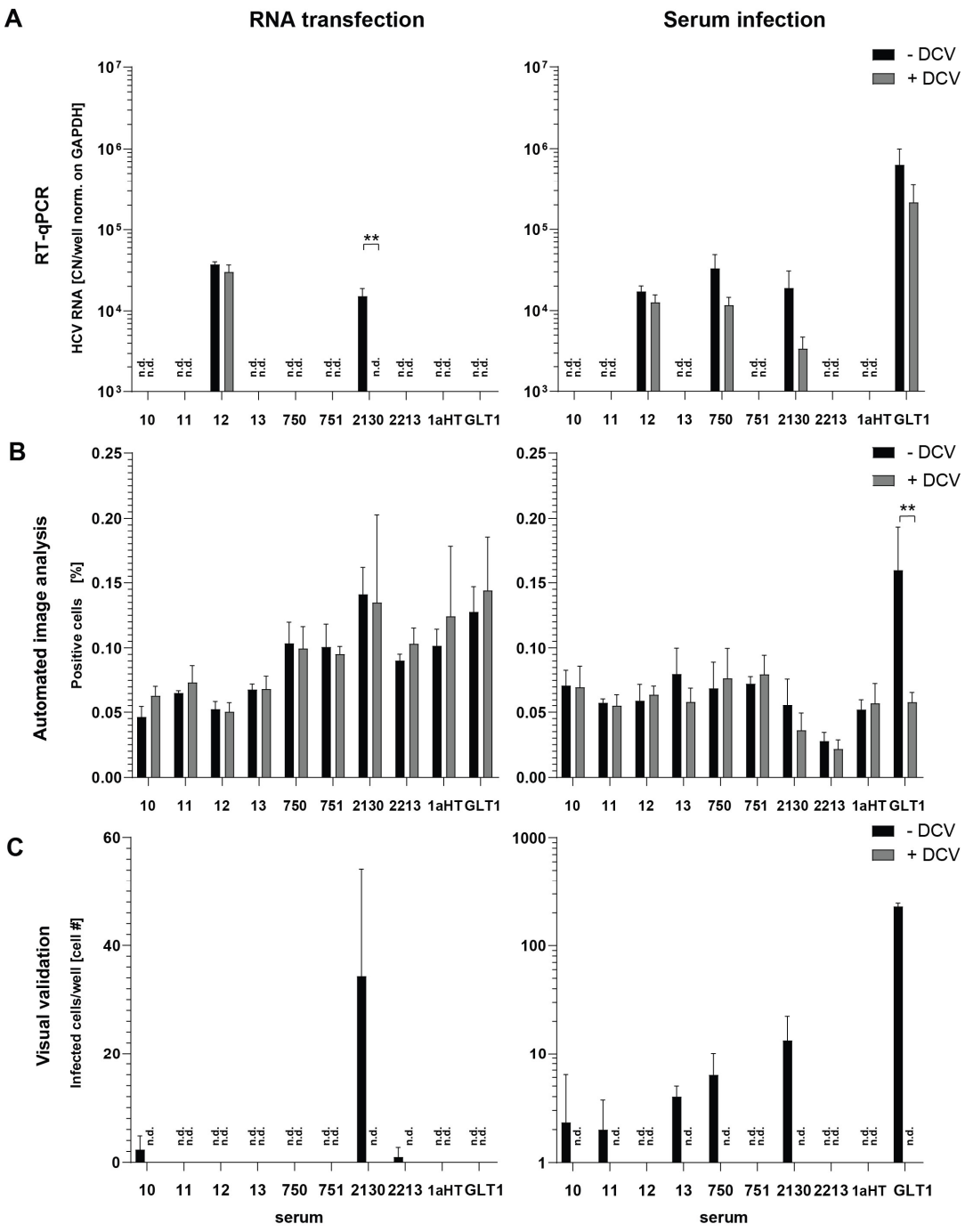

Figure 6. Results of RNA transfection in comparison to serum infection. 10 patient sera were tested using RNA transfection and serum infection in parallel. All samples were harvested after 72 h, treatment with DCV served as negative control. Samples were analysed via RT-qPCR (A), AIA (B) and with AIA followed by visual validation (C). Values are shown as means of three biological replicates and were measured in technical triplicates in RT-qPCR. Data of the serum infection assay of sera 2130, 2213, AU and GLT1 was taken from Figure 4 for better comparison. n.d.: not detectable. *P < 0.05, **P < 0.01 (unpaired two-tailed Student's t-test).

Discussion

In this study, sera mostly from gt1b HCV infected patients were tested on their capacity to establish successful RNA replication in Huh7-Lunet C/M/S cells. A newly established quantitative image-based analysis with visual validation proved to be virtually free of any background, allowing a robust detection even of single infection events.

Preprints.org (www.preprints.org) | NOT PEER-REVIEWED | Posted: 25 October 2024 doi:10.20944/preprints202410.2010.v1

In this study, RT-qPCR failed to generate statistically significant differences compared to DCV-treatment, which is an essential control, likely due to high background of cell-associated virions. This view is supported by the reduced background observed upon electroporation of purified viral RNA. A potential reason for high background might be the spin-infection, which was part of our protocol [21], but not used in other studies [25,26]. We therefore used an alternative detection method based on viral protease activity [34]. This system is well established in the context of HCVcc infection [45,46], also in combination with automated image analysis [24,34] and in a proof-of-concept to detect infection of serum-born virus [21]. Due to the expectedly low number of infection events, imaging of whole wells combined with automated image analysis were essential components for a reproducible analysis pipeline for serum infection. In contrast to the RT-qPCR, background arose from false positive assignments of nuclear GFP signals, e.g. in areas with high cell density, which could be reduced to 0.02% by iterative training of the software. Importantly, background could be completely eliminated by visual control, generating a robust assay allowing the unequivocal detection of even single infection events with reasonable effort. The background might be further reduced by alternative reporter systems based on split-GFP [47].

Since our focus was on testing rather rare high-titer gt1b sera, we mainly had to rely on historical samples. In total, infection events were detectable in 15 out of 34 sera, with a significant correlation of high titers and successful infection. Still, there was no clear threshold titer and titers did not correlate at all with number of infection events. The variability observed was likely due to unknown storage conditions/freeze thaw cycles [48] and the presence of neutralizing antibodies (reviewed in [49]). Among those sera with known storage history lacking freeze-thaw cycles (Table 2) 4 out of 6 gave rise to infections, despite comparably low titers, suggesting that the success rate might be higher in freshly acquired samples. Post-transplant sera also had a higher than average success rate (8/11, versus 7/24 not-transplant sera), which could be due high average titers, lack of neutralizing antibodies and the presence of variants with higher fitness. Previous studies have shown that HCV reinfection after liver transplantation results in a reduction of HCV genome sequence variety [30,50] which can be associated with increased cell entry competence [51,52]. Interestingly, the GLT1 patient serum showed the highest number of infection events, and has been shown to replicate with far higher efficiency than common gt1b isolates like Con1 [24], pointing towards selection for increased RNA replication fitness after liver transplantation (LTx), with yet unknown sequence determinants.

We focused our analysis on gt1b sera, since previous studies have shown that SEC14L2 expression as well as PCi treatment work most efficiently/exclusively in this context. PCi treatment mimics the mode of action of distinct classes of adaptive mutations [21], but since only gt1b isolates are capable of replicating with a single adaptive mutation, this measure is not sufficient for other genotypes. SEC14L2 acts pan-genotypically in the context of selectable genomes [25], but also here efficiency dramatically differs among genotypes, again with gt1b being most efficiently stimulated in transient replication assays [26]. We combined both measures and carefully optimized them here, due to additive effects observed with reporter replicons [24]. We did not further evaluate the sole use of SEC14L2 as in previous studies [25,26] due to limited amounts of available sera. However, we confirmed that even combined use of PCi and SEC14L2 was very inefficient in enhancing replication of cloned gt1a and gt3a wt isolates TNwt and DBNwt, respectively [19,20] and further failed to detect infection based on a gt1a post-transplant serum. Still, previous studies succeeded in infecting SEC14L2 expressing cells, based on gt3a sera [25,26]. This might either be due to differences in SEC14L2 expression levels, or due to the presence of specific high replicator isolates in the high-titer post-transplant sera used [25], comparable to our GLT1 isolate [21,24]. A better understanding of determinants of cell culture adaptation in Huh7 cells or the establishment of alternative cell culture models is required to allow robust serum infections beyond gt1b.

To overcome the limited availability of high titer sera and to avoid factors interfering with serum infection like neutralizing antibodies, damaged viral particles, cytotoxic serum components, etc., we further evaluated the possibility to transfect viral RNA purified from serum. However, already the validation based on in vitro transcribed viral genomes demonstrated the need for more than 10^7 viral genomes for detection of HCV positive cells, probably due to the accessibility of naked viral RNA to

Preprints.org (www.preprints.org) | NOT PEER-REVIEWED | Posted: 25 October 2024 doi:10.20944/preprints202410.2010.v1

RNases during transfection. Still, the principle feasibility of transfection of purified RNA from serum offers the opportunity for upscaling. We so far failed to enrich viral RNA from larger volumes by ultracentrifugation, probably due to the heterogeneous density of HCV particles in serum [53]. A careful optimization of virus purification and concentration methods, e.g. using aqueous two-phase systems, might enable efficient purification of viral RNA from large serum volumes [54].

DAAs have revolutionized HCV therapies, offering save and effective treatment options for almost all patients. However, some viral isolates have been identified with an enhanced amount of clinically relevant RAS conferring resistance to current drug regimens [55–58] and new HCV subtypes, mostly deriving from sub-Saharan Africa, revealed a higher prevalence of clinically relevant RAS, leading to an enhanced rate of treatment failure in these patients [59]. Here, a serum based infection assay could help to find personalized treatment options including the use of drugs with so far unpredictable response pattern like Legalon-SIL [37,60]. Another possible application of serum-infection assays is in the characterization of neutralizing antibody responses in vaccine development, which are so far based on collections of prototype isolates [61,62], lacking genetic intra-host diversity (reviewed in [63]).

Overall, our study established an experimental pipeline facilitating HCV infections based on patient sera, which might be helpful in developing personalized treatment regimens in hard to cure patients and in vaccine development.

AUTHOR CONTRIBUTIONS: Conceptualization, NS and VoL; Funding acquisition, VoL; Investigation, NS; Methodology, NS, PR, CH and ViL; Project administration, VoL; Resources, CNH, RT, JD, CS, PS, UM and SPdP; Software, ViL; Supervision, VoL; Visualization, NS; Writing – original draft, NS and VoL; Writing – review & editing, all authors.

FUNDING INFORMATION: This project was funded by grants from the Deutsche Forschungsgemeinschaft, project numbers 519777725 (to VoL) and 272983813 (to VoL, CNH and RT). VoL, JD and CS were supported by the German Center for Infection Research (DZIF), TTU 05.821. NS was supported by a stipend from the DZIF academy.

ACKNOWLEDGEMENTS: We thank R. Klein and U. Herian for excellent technical assistance. We are grateful to R. De Francesco for providing the CKIα inhibitor H479 and J. Botyanszki for compound PI4KA-F1. We thank T. Wakita for the JFH-1 isolate, J. Bukh for plasmids encoding the DBN3a WT and TN WT isolates. We also thank the Infectious Disease Imaging Platform (IDIP) headed by V. Laketa for facility use.

CONFLICTS OF INTEREST: The authors have nothing to disclose.

References

1. Hajarizadeh B, Grebely J, Dore GJ. 2013. Epidemiology and natural history of HCV infection. Nat Rev Gastroenterol Hepatol doi:nrgastro.2013.107 [pii];10.1038/nrgastro.2013.107 [doi].
2. Thein H-H, Yi Q, Dore GJ, Krahn MD. 2008. Estimation of stage-specific fibrosis progression rates in chronic hepatitis C virus infection: A meta-analysis and meta-regression. Hepatology 48:418-431.
3. Westbrook RH, Dusheiko G. 2014. Natural history of hepatitis C. Journal of Hepatology 61:S58-S68.
4. Borgia SM, Hedskog C, Parhy B, Hyland RH, Stamm LM, Brainard DM, Subramanian MG, McHutchison JG, Mo H, Svarovskaia E, Shafran SD. 2018. Identification of a Novel Hepatitis C Virus Genotype From Punjab, India: Expanding Classification of Hepatitis C Virus Into 8 Genotypes. J Infect Dis 218:1722-1729.
5. Bukh J, Miller RH, Purcell RH. 1995. Genetic heterogeneity of hepatitis C virus: quasispecies and genotypes. Semin Liver Dis 15:41-63.
6. Simmonds P, Bukh J, Combet C, Deleage G, Enomoto N, Feinstone S, Halfon P, Inchauspe G, Kuiken C, Maertens G, Mizokami M, Murphy DG, Okamoto H, Pawlotsky JM, Penin F, Sablon E, Shin I, Stuyver LJ, Thiel HJ, Viazov S, Weiner AJ, Widell A. 2005. Consensus proposals for a unified system of nomenclature of hepatitis C virus genotypes. Hepatology 42:962-973.
7. Martell M, Esteban JI, Quer J, Genesca J, Weiner A, Esteban R, Guardia J, Gomez J. 1992. Hepatitis C virus (HCV) circulates as a population of different but closely related genomes: quasispecies nature of HCV genome distribution. J Virol 66:3225-3229.
8. Sarrazin C, Zimmermann T, Berg T, Neumann UP, Schirmacher P, Schmidt H, Spengler U, Timm J, Wedemeyer H, Wirth S, Zeuzem S. 2018. [Prophylaxis, diagnosis and therapy of hepatitis-C-virus (HCV)

Preprints.org (www.preprints.org) | NOT PEER-REVIEWED | Posted: 25 October 2024 doi:10.20944/preprints202410.2010.v1

infection: the German guidelines on the management of HCV infection - AWMF-Register-No.: 021/012]. Z Gastroenterol 56:756-838.
9. Bartenschlager R, Baumert TF, Bukh J, Houghton M, Lemon SM, Lindenbach BD, Lohmann V, Moradpour D, Pietschmann T, Rice CM, Thimme R, Wakita T. 2018. Critical challenges and emerging opportunities in hepatitis C virus research in an era of potent antiviral therapy: Considerations for scientists and funding agencies. Virus Research 248:53-62.
10. Pawlotsky J-M. 2016. Hepatitis C Virus Resistance to Direct-Acting Antiviral Drugs in Interferon-Free Regimens. Gastroenterology 151:70-86.
11. Dietz J, Lohmann V. 2023. Therapeutic preparedness: DAA-resistant HCV variants in vitro and in vivo. Hepatology 78:385-387.
12. Lohmann V, Korner F, Koch J, Herian U, Theilmann L, Bartenschlager R. 1999. Replication of subgenomic hepatitis C virus RNAs in a hepatoma cell line. Science 285:110-113.
13. Lohmann V, Hoffmann S, Herian U, Penin F, Bartenschlager R. 2003. Viral and cellular determinants of hepatitis C virus RNA replication in cell culture. J Virol 77:3007-3019.
14. Kato T, Date T, Miyamoto M, Furusaka A, Tokushige K, Mizokami M, Wakita T. 2003. Efficient replication of the genotype 2a hepatitis C virus subgenomic replicon. Gastroenterology 125:1808-1817.
15. Lindenbach BD, Evans MJ, Syder AJ, Wolk B, Tellinghuisen TL, Liu CC, Maruyama T, Hynes RO, Burton DR, McKeating JA, Rice CM. 2005. Complete replication of hepatitis C virus in cell culture. Science 309:623-626.
16. Pietschmann T, Kaul A, Koutsoudakis G, Shavinskaya A, Kallis S, Steinmann E, Abid K, Negro F, Dreux M, Cosset FL, Bartenschlager R. 2006. Construction and characterization of infectious intragenotypic and intergenotypic hepatitis C virus chimeras. Proc Natl Acad Sci U S A 103:7408-7413.
17. Pham LV, Ramirez S, Gottwein JM, Fahnoe U, Li YP, Pedersen J, Bukh J. 2018. HCV Genotype 6a Escape From and Resistance to Velpatasvir, Pibrentasvir, and Sofosbuvir in Robust Infectious Cell Culture Models. Gastroenterology 154:2194-2208 e12.
18. Yi M, Villanueva RA, Thomas DL, Wakita T, Lemon SM. 2006. Production of infectious genotype 1a hepatitis C virus (Hutchinson strain) in cultured human hepatoma cells. Proc Natl Acad Sci U S A 103:2310-5.
19. Li YP, Ramirez S, Jensen SB, Purcell RH, Gottwein JM, Bukh J. 2012. Highly efficient full-length hepatitis C virus genotype 1 (strain TN) infectious culture system. Proc Natl Acad Sci U S A 109:19757-19762.
20. Ramirez S, Mikkelsen LS, Gottwein JM, Bukh J. 2016. Robust HCV Genotype 3a Infectious Cell Culture System Permits Identification of Escape Variants With Resistance to Sofosbuvir. Gastroenterology 151:973-985.e2.
21. Harak C, Meyrath M, Romero-Brey I, Schenk C, Gondeau C, Schult P, Esser-Nobis K, Saeed M, Neddermann P, Schnitzler P, Gotthardt D, Perez-Del-Pulgar S, Neumann-Haefelin C, Thimme R, Meuleman P, Vondran FW, De FR, Rice CM, Bartenschlager R, Lohmann V. 2016. Tuning a cellular lipid kinase activity adapts hepatitis C virus to replication in cell culture. Nat Microbiol 2:16247.
22. Ilboudo A, Nault J-C, Dubois-Pot-Schneider H, Corlu A, Zucman-Rossi J, Samson M, Le Seyec J. 2014. Overexpression of phosphatidylinositol 4-kinase type IIIα is associated with undifferentiated status and poor prognosis of human hepatocellular carcinoma. BMC Cancer 14:7.
23. Neddermann P, Quintavalle M, Di Pietro C, Clementi A, Cerretani M, Altamura S, Bartholomew L, De Francesco R. 2004. Reduction of hepatitis C virus NS5A hyperphosphorylation by selective inhibition of cellular kinases activates viral RNA replication in cell culture. J Virol 78:13306-13314.
24. Heuss C, Rothhaar P, Burm R, Lee JY, Ralfs P, Haselmann U, Stroh LJ, Colasanti O, Tran CS, Schafer N, Schnitzler P, Merle U, Bartenschlager R, Patel AH, Graw F, Krey T, Laketa V, Meuleman P, Lohmann V. 2022. A Hepatitis C virus genotype 1b post-transplant isolate with high replication efficiency in cell culture and its adaptation to infectious virus production in vitro and in vivo. PLoS Pathog 18:e1010472.
25. Saeed M, Andreo U, Chung HY, Espiritu C, Branch AD, Silva JM, Rice CM. 2015. SEC14L2 enables pan-genotype HCV replication in cell culture. Nature 524:471-475.
26. Costa R, Todt D, Zapatero-Belinchon F, Schenk C, Anastasiou OE, Walker A, Hertel B, Timmer L, Bojkova D, Ruckert M, Sarrazin C, Timm J, Lohmann V, Manns MP, Steinmann E, von Hahn T, Ciesek S. 2019. SEC14L2, a lipid-binding protein, regulates HCV replication in culture with inter- and intra-genotype variations. J Hepatol 70:603-614.
27. Vrolijk JM, Kaul A, Hansen BE, Lohmann V, Haagmans BL, Schalm SW, Bartenschlager R. 2003. A replicon-based bioassay for the measurement of interferons in patients with chronic hepatitis C. J Virol Methods 110:201-209.
28. Jo J, Aichele U, Kersting N, Klein R, Aichele P, Bisse E, Sewell AK, Blum HE, Bartenschlager R, Lohmann V, Thimme R. 2009. Analysis of CD8+ T-cell-mediated inhibition of hepatitis C virus replication using a novel immunological model. Gastroenterology 136:1391-1401.
29. Frese M, Barth K, Kaul A, Lohmann V, Schwarzle V, Bartenschlager R. 2003. Hepatitis C virus RNA replication is resistant to tumour necrosis factor-alpha. J Gen Virol 84:1253-1259.

Preprints.org (www.preprints.org) | NOT PEER-REVIEWED | Posted: 25 October 2024 doi:10.20944/preprints202410.2010.v1

30. Gambato M, Gregori J, Quer J, Koutsoudakis G, González P, Caro-Pérez N, García-Cehic D, García-González N, González-Candelas F, Esteban JI, Crespo G, Navasa M, Forns X, Pérez-del-Pulgar S. 2019. Hepatitis C virus intrinsic molecular determinants may contribute to the development of cholestatic hepatitis after liver transplantation. Journal of General Virology 100:63-68.
31. Berg S, Kutra D, Kroeger T, Straehle CN, Kausler BX, Haubold C, Schiegg M, Ales J, Beier T, Rudy M, Eren K, Cervantes JI, Xu B, Beuttenmueller F, Wolny A, Zhang C, Koethe U, Hamprecht FA, Kreshuk A. 2019. ilastik: interactive machine learning for (bio)image analysis. Nat Methods 16:1226-1232.
32. Bojjireddy N, Botyanszki J, Hammond G, Creech D, Peterson R, Kemp DC, Snead M, Brown R, Morrison A, Wilson S, Harrison S, Moore C, Balla T. 2014. Pharmacological and genetic targeting of the PI4KA enzyme reveals its important role in maintaining plasma membrane phosphatidylinositol 4-phosphate and phosphatidylinositol 4,5-bisphosphate levels. J Biol Chem 289:6120-6132.
33. Koutsoudakis G, Herrmann E, Kallis S, Bartenschlager R, Pietschmann T. 2007. The level of CD81 cell surface expression is a key determinant for productive entry of hepatitis C virus into host cells. J Virol 81:588-598.
34. Jones CT, Catanese MT, Law LMJ, Khetani SR, Syder AJ, Ploss A, Oh TS, Schoggins JW, MacDonald MR, Bhatia SN, Rice CM. 2010. Real-time imaging of hepatitis C virus infection using a fluorescent cell-based reporter system. Nature Biotechnology 28:167-171.
35. Bartenschlager R, Lohmann V, Penin F. 2013. The molecular and structural basis of advanced antiviral therapy for hepatitis C virus infection. Nat Rev Microbiol 11:482-496.
36. Ferenci P, Scherzer TM, Kerschner H, Rutter K, Beinhardt S, Hofer H, Schöniger–Hekele M, Holzmann H, Steindl–Munda P. 2008. Silibinin Is a Potent Antiviral Agent in Patients With Chronic Hepatitis C Not Responding to Pegylated Interferon/Ribavirin Therapy. Gastroenterology 135:1561-1567.
37. Esser-Nobis K, Romero-Brey I, Ganten TM, Gouttenoire J, Harak C, Klein R, Schemmer P, Binder M, Schnitzler P, Moradpour D, Bartenschlager R, Polyak SJ, Stremmel W, Penin F, Eisenbach C, Lohmann V. 2013. Analysis of hepatitis C virus resistance to silibinin in vitro and in vivo points to a novel mechanism involving nonstructural protein 4B. Hepatology 57:953-963.
38. Coelmont L, Hanoulle X, Chatterji U, Berger C, Snoeck J, Bobardt M, Lim P, Vliegen I, Paeshuyse J, Vuagniaux G, Vandamme AM, Bartenschlager R, Gallay P, Lippens G, Neyts J. 2010. DEB025 (Alisporivir) inhibits hepatitis C virus replication by preventing a cyclophilin A induced cis-trans isomerisation in domain II of NS5A. PLoS One 5:e13687.
39. Fernandes F, Ansari I-uH, Striker R. 2010. Cyclosporine Inhibits a Direct Interaction between Cyclophilins and Hepatitis C NS5A. PLOS ONE 5:e9815.
40. Hanoulle X, Badillo A, Wieruszeski JM, Verdegem D, Landrieu I, Bartenschlager R, Penin F, Lippens G. 2009. Hepatitis C virus NS5A protein is a substrate for the peptidyl-prolyl cis/trans isomerase activity of cyclophilins A and B. J Biol Chem 284:13589-13601.
41. Wagoner J, Negash A, Kane OJ, Martinez LE, Nahmias Y, Bourne N, Owen DM, Grove J, Brimacombe C, McKeating JA, Pecheur EI, Graf TN, Oberlies NH, Lohmann V, Cao F, Tavis JE, Polyak SJ. 2010. Multiple effects of silymarin on the hepatitis C virus lifecycle. Hepatology 51:1912-1921.
42. Guedj J, Dahari H, Pohl RT, Ferenci P, Perelson AS. 2012. Understanding silibinin's modes of action against HCV using viral kinetic modeling. J Hepatol 56:1019-1024.
43. Blaising J, Lévy PL, Gondeau C, Phelip C, Varbanov M, Teissier E, Ruggiero F, Polyak SJ, Oberlies NH, Ivanovic T, Boulant S, Pécheur EI. 2013. Silibinin inhibits hepatitis C virus entry into hepatocytes by hindering clathrin-dependent trafficking. Cell Microbiol 15:1866-82.
44. Wu Y, Liao Q, Yang R, Chen X, Chen X. 2011. A novel luciferase and GFP dual reporter virus for rapid and convenient evaluation of hepatitis C virus replication. Virus Research 155:406-414.
45. Ren Q, Li C, Yuan P, Cai C, Zhang L, Luo GG, Wei W. 2015. A Dual-Reporter System for Real-Time Monitoring and High-throughput CRISPR/Cas9 Library Screening of the Hepatitis C Virus. Scientific Reports 5:8865.
46. Xiao F, Fofana I, Heydmann L, Barth H, Soulier E, Habersetzer F, Doffoël M, Bukh J, Patel AH, Zeisel MB, Baumert TF. 2014. Hepatitis C Virus Cell-Cell Transmission and Resistance to Direct-Acting Antiviral Agents. PLOS Pathogens 10:e1004128.
47. Zhao F, Zhao T, Deng L, Lv D, Zhang X, Pan X, Xu J, Long G. 2017. Visualizing the Essential Role of Complete Virion Assembly Machinery in Efficient Hepatitis C Virus Cell-to-Cell Transmission by a Viral Infection-Activated Split-Intein-Mediated Reporter System. Journal of Virology 91:10.1128/jvi.01720-16.
48. Andreo U, de Jong YP, Scull MA, Xiao JW, Vercauteren K, Quirk C, Mommersteeg MC, Bergaya S, Menon A, Fisher EA, Rice CM. 2017. Analysis of Hepatitis C Virus Particle Heterogeneity in Immunodeficient Human Liver Chimeric fah-/- Mice. Cellular and Molecular Gastroenterology and Hepatology 4:405-417.
49. Ball JK, Tarr AW, McKeating JA. 2014. The past, present and future of neutralizing antibodies for hepatitis C virus. Antiviral Res 105:100-11.
50. Demetris AJ. 2009. Evolution of hepatitis C virus in liver allografts. Liver Transplantation 15:S35-S41.

Preprints.org (www.preprints.org) | NOT PEER-REVIEWED | Posted: 25 October 2024 doi:10.20944/preprints202410.2010.v1

51. Fafi-Kremer S, Fofana I, Soulier E, Carolla P, Meuleman P, Leroux-Roels G, Patel AH, Cosset F-L, Pessaux P, Doffoël M, Wolf P, Stoll-Keller F, Baumert TF. 2010. Viral entry and escape from antibody-mediated neutralization influence hepatitis C virus reinfection in liver transplantation. Journal of Experimental Medicine 207:2019-2031.
52. Schvoerer E, Soulier E, Royer C, Renaudin A-C, Thumann C, Fafi-Kremer S, Brignon N, Doridot S, Meyer N, Pinson P, Ellero B, Woehl-Jaegle M-L, Meyer C, Wolf P, Zachary P, Baumert T, Stoll-Keller F. 2007. Early Evolution of Hepatitis C Virus (HCV) Quasispecies after Liver Transplant for HCV-Related Disease. The Journal of Infectious Diseases 196:528-536.
53. Thomssen R, Bonk S, Thiele A. 1993. Density heterogeneities of hepatitis C virus in human sera due to the binding of beta-lipoproteins and immunoglobulins. Med Microbiol Immunol Berl 182:329-334.
54. Kim H, Yi J, Yu J, Park J, Jang SK. 2022. A Simple and Effective Method to Concentrate Hepatitis C Virus: Aqueous Two-Phase System Allows Highly Efficient Enrichment of Enveloped Viruses. Viruses 14.
55. Bagaglio S, Messina E, Hasson H, Galli A, Uberti-Foppa C, Morsica G. 2019. Geographic Distribution of HCV-GT3 Subtypes and Naturally Occurring Resistance Associated Substitutions. Viruses 11.
56. Fernandez-Antunez C, Wang K, Fahnøe U, Mikkelsen LS, Gottwein JM, Bukh J, Ramirez S. 2023. Characterization of multi-DAA resistance using a novel hepatitis C virus genotype 3a infectious culture system. Hepatology 78:621-636.
57. Sarrazin C. 2021. Treatment failure with DAA therapy: Importance of resistance. Journal of Hepatology 74:1472-1482.
58. Smith D, Magri A, Bonsall D, Ip CLC, Trebes A, Brown A, Piazza P, Bowden R, Nguyen D, Ansari MA, Simmonds P, Barnes E. 2019. Resistance analysis of genotype 3 hepatitis C virus indicates subtypes inherently resistant to nonstructural protein 5A inhibitors. Hepatology 69:1861-1872.
59. Vo-Quang E, Soulier A, Ndebi M, Rodriguez C, Chevaliez S, Leroy V, Fourati S, Pawlotsky JM. 2023. Virological characterization of treatment failures and retreatment outcomes in patients infected with "unusual" HCV genotype 1 subtypes. Hepatology 78:607-620.
60. Mariño Z, Crespo G, D'Amato M, Brambilla N, Giacovelli G, Rovati L, Costa J, Navasa M, Forns X. 2013. Intravenous silibinin monotherapy shows significant antiviral activity in HCV-infected patients in the peri-transplantation period. J Hepatol 58:415-20.
61. Bankwitz D, Bahai A, Labuhn M, Doepke M, Ginkel C, Khera T, Todt D, Stroh LJ, Dold L, Klein F, Klawonn F, Krey T, Behrendt P, Cornberg M, McHardy AC, Pietschmann T. 2021. Hepatitis C reference viruses highlight potent antibody responses and diverse viral functional interactions with neutralising antibodies. Gut 70:1734-1745.
62. Salas JH, Urbanowicz RA, Guest JD, Frumento N, Figueroa A, Clark KE, Keck Z, Cowton VM, Cole SJ, Patel AH, Fuerst TR, Drummer HE, Major M, Tarr AW, Ball JK, Law M, Pierce BG, Foung SKH, Bailey JR. 2022. An Antigenically Diverse, Representative Panel of Envelope Glycoproteins for Hepatitis C Virus Vaccine Development. Gastroenterology 162:562-574.
63. Cox AL. 2020. Challenges and Promise of a Hepatitis C Virus Vaccine. Cold Spring Harb Perspect Med 10.

Disclaimer/Publisher's Note: The statements, opinions and data contained in all publications are solely those of the individual author(s) and contributor(s) and not of MDPI and/or the editor(s). MDPI and/or the editor(s) disclaim responsibility for any injury to people or property resulting from any ideas, methods, instructions or products referred to in the content.